Cyclotron resonance phenomena in a pure electron plasma*

Roy W. Gould† and Michael A. LaPointe
Department of Applied Physics, California Institute of Technology, Pasadena, California 91125

(Received 25 November 1991; accepted 29 January 1992)

An experiment designed to elucidate the features of cyclotron resonance in a rotating cylindrical pure electron plasma column is described. The density is well below the Brillouin limit and varies with radius, as does the rotational angular velocity. Thus the steady state is not the rigid-rotor equilibrium which is frequently studied theoretically. The readily observed modes are found to have $k_z \approx 0$ and $m=1,2,3,4...$ ($e^{ik_z z+im\theta}$) with frequencies which are within a few percent of the cyclotron frequency (140 MHz). A single $m=1$ mode is found that is downshifted from the cyclotron frequency by an amount equal to the $m=1$ diocotron frequency. For each of the higher m values, bands of closely spaced discrete modes are found which are upshifted from the cyclotron frequency by the Doppler effect of rotation. The bands of discrete modes are explained as radially trapped azimuthally propagating Bernstein modes in a rotating plasma and approximate theories for these modes are outlined. By comparing the results with experiments, plasma parameters such as the ratio of Larmor radius to plasma scale length, the central rotation frequency, and the ratio of peak to average density can be inferred.

I. INTRODUCTION

Non-neutral plasmas have been the subject of extensive study during the past decade.[1,2] Low-frequency phenomena such as approach to equilibrium,[3] stability of low-frequency modes,[4] and transport[5] have been studied experimentally. High-frequency phenomena in non-neutral plasmas have not been studied experimentally. However, cyclotron resonance is used for high precision mass spectrometry,[6] but generally at densities where plasma effects are unimportant.[7] Plasma effects on cyclotron resonance, e.g., upper-hybrid resonance, have been studied extensively in neutral plasmas, as have cyclotron harmonic effects.[8] It has also been shown theoretically how some of these effects should carry over to non-neutral plasmas in the special case of rigid-rotor equilibria.[9,2] The rotation of non-neutral plasmas causes significant differences from the neutral plasma phenomena, and the existence of an angular velocity profile causes significant differences from the rigid-rotor predictions. In this paper we report new high-frequency measurements of plasma effects on cyclotron resonance in a pure electron plasma column which demonstrate the effects of plasma rotation and the existence of radially trapped Bernstein waves,[10] similar in some respects to the Buchsbaum–Hasegawa modes in a neutral plasma.[11] We also sketch out simple explanations of the phenomena.

II. EXPERIMENT

In this experiment we employ the Penning trap configuration, exploited so successfully by the San Diego group. Electrons are contained radially by a magnetic field, which results in rotation about the axis of symmetry, and axially by electrostatic potentials. Electrons are injected (from a spiral filament), trapped, then dumped in a repetitive cycle.[12] Figure 1 is a schematic drawing of the experiment and the parameters of our device are shown in Table I. During the trapping time, the electron density decays due to causes that are not fully understood.[5] We exploit this density decay in our measurements to provide a density scan. A cylindrical non-neutral plasma column has a low-frequency $m=1$ mode, generally referred to as the diocotron mode,[13] whose frequency is given by

$$\omega_d \equiv \langle \omega_p^2 \rangle / 2\omega_c, \tag{1}$$

where $\langle \omega_p^2 \rangle = \langle n_0 \rangle e^2/\epsilon_0 m_e$ is the square of the plasma frequency, averaged over the plasma cross section, out to the surrounding conductor, and $\omega_c = eB/m_e$ is the cyclo-

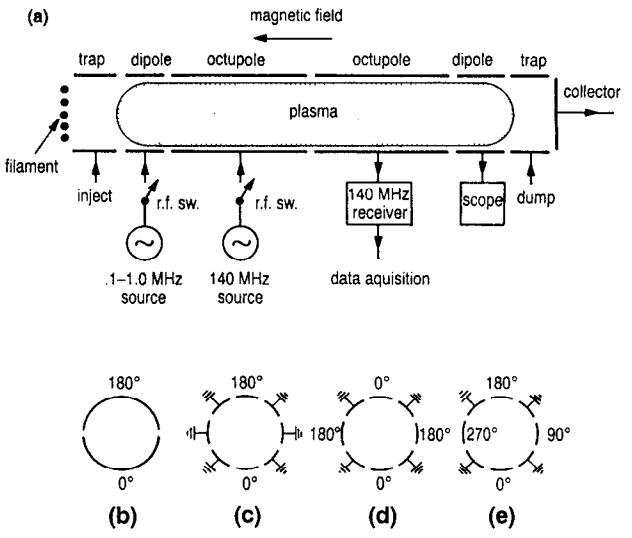

FIG. 1. Schematic of the experimental device. (a) Cylindrical electrode structure and instrumentation. (b)–(e) illustrate possible phasings of the dipole and octupole sections.

*Paper 1I4, Bull. Am. Phys. Soc. **36**, 2270 (1991).
†Invited speaker.

 0899-8213/92/072038-06$04.00

TABLE I. Pure electron plasma experimental parameters.

Magnetic field	~50 G
Field uniformity	±0.015%
Electron density	$<5\times10^6$ cm^{-3}
Electron temperature	1–2 eV
Cylinder radius	2.5 cm
Trap length	40 cm
Trap duration	200 msec (typical)
Repetition rate	5 Hz (typical)
Cyclotron frequency	~140 MHz
Plasma frequency	<20 MHz
Rotation frequency	<2 MHz
Axial bounce frequency	1–2 MHz
Diocotron frequency	<1 MHz
Larmor radius	~1 mm
Debye length	>7 mm

tron frequency. Here ω_d is proportional to the electron line density. We also note that, in general, the rotational angular velocity $\omega_0(r)=E_r(r)/rB$ of a non-neutral plasma varies with radius in a way which depends upon the density profile through the relationship[13] $(1/r)d[r^2\omega_0(r)]/dr = \omega_p^2(r)/\omega_c$. It is convenient for our later discussions to introduce normalized angular velocity and density profiles, $f(r)$ and $g(r)$, as follows: $\omega_p^2(r)=\omega_p^2(0)f(r)$ and $\omega_0(r)=\omega_0(0)g(r)$. When the density profile decreases monotonically with radius, so does the angular velocity profile, as illustrated by the example of Fig. 2. Near the axis we assume that $f(r)$ has the form $1-(r/a)^2$, where a is the scale length of the density profile. This gives an angular velocity profile $g(r)=1-0.5(r/a)^2$. In the discussion of our results we use the monotonic feature of the angular velocity profile.

The cylindrical electrode structure is segmented azimuthally and axially, with coaxial feeds to each segment so as to be able to apply rf electric fields to the plasma of a known spatial variation. As shown in Fig. 1(a), there are two octupole sections, two dipole sections, and two cylindrical trap electrodes symmetrically disposed about the midplane. By applying rf potentials of differing phases to different sections of the octupoles it is possible to emphasize different circular harmonics ($m=1,2,3...$ for $e^{im\theta}$). For example, driving one electrode only excites all harmonics up to $m=7$ with diminishing amplitude. The configuration of Fig. 1(c) excites $m=1,3,5,...$ and that of Fig. 1(d) excites $m=2,6,...$. Configuration 1(e) creates mainly an $m=1$ rotating electric field. Only $m>0$ circular harmonics give right circularly polarized electric fields which can drive electron cyclotron resonance.

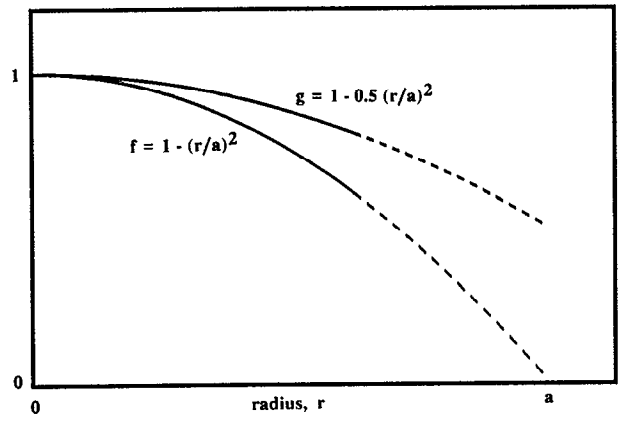

FIG. 2. Normalized radial density profile, $f(r)$, and corresponding normalized angular velocity profile, $g(r)$.

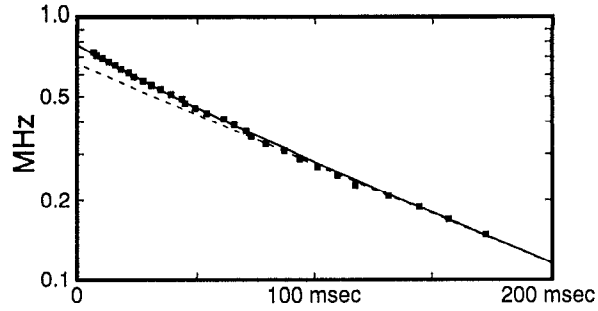

FIG. 3. Decay of the mean plasma density versus time. $f_d=\langle f_p^2\rangle/2f_c$ is plotted.

In this experiment, one octupole section is driven from a source of about 140 MHz and the second octupole section is connected to a 140 MHz receiver and data acquisition system so as to form a *transmission* system. Transmission peaks occur when the conditions (density and magnetic field) in the plasma are such that a normal mode of the plasma exists at the source frequency. During the trap period the density decays as shown in Fig. 3. On successive trap cycles we increment the magnetic field by a small amount. A complete scan requires 100–200 cycles. In this way we are able to make a two-dimensional scan in density and magnetic field. Figure 4 shows such a scan in which various resonances of the column are evident. Through the use of various phasings of the octupole sections described previously, we are able to identify the m numbers of the modes shown in Fig. 4. All of the modes shown correspond to $k_z=0$. As may be seen from this figure, there is only one $m=1$ mode and it occurs for $f<f_c$. For each m greater than 1, there are *sets* of modes occurring for $f>f_c$. Each of the various modes tends toward the cyclotron frequency as the density decays, suggesting that the *differences* from f_c are proportional to density. Later, we will see that this is the case.

III. THE DIPOLE MODE, $m=1$

From Fig. 4 we see a single dipole mode whose separation from the cyclotron frequency decreases with decreasing density. To quantify this relationship we have measured, nearly simultaneously, the frequency of the $m=1$ cyclotron mode and the frequency of the $m=1$ diocotron mode, the latter giving the mean density. To measure the cyclotron mode frequency at a particular time in the plasma decay, we apply a short burst, typically 200 μsec, of rf to one octupole section and adjust its frequency so as to maximize the rf amplitude received by the second octupole section at the end of the burst. We also measure

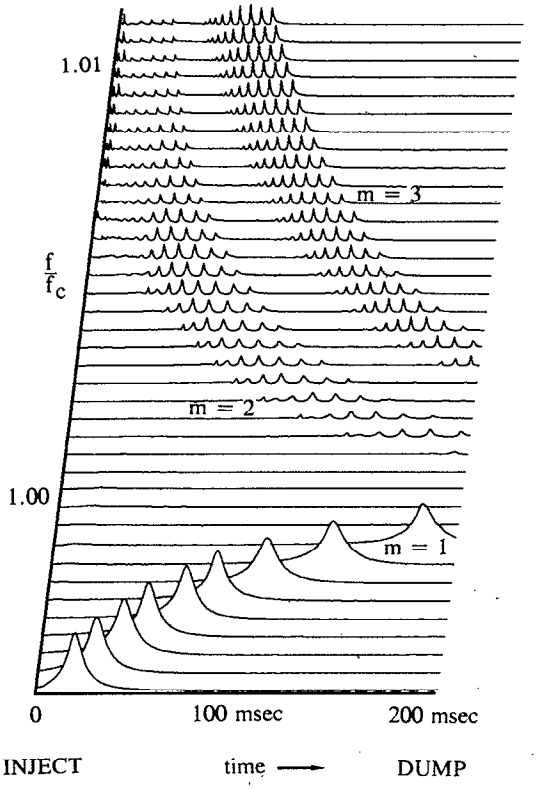

FIG. 4. Transmission between octupole sections showing normal modes of the plasma. The magnetic field is decremented on successive traces. For clarity every third trace is displayed. The $m=4$ resonances are too small to be seen in this display.

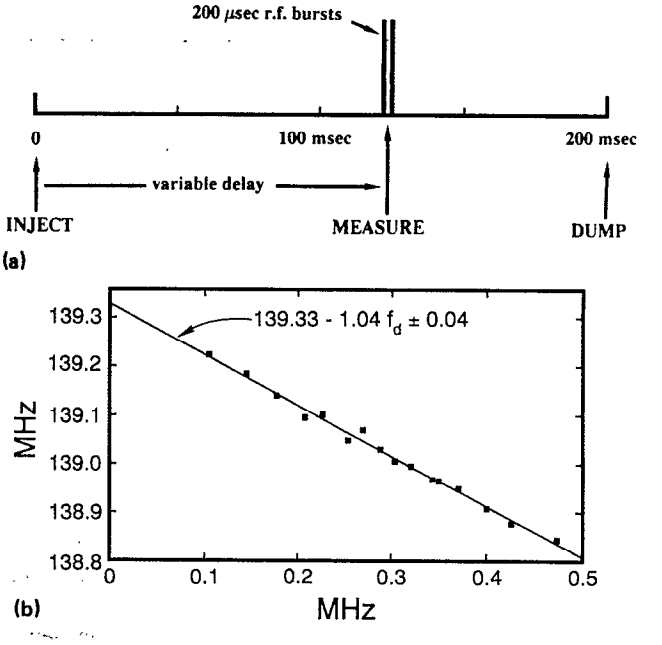

FIG. 5. Measurement of the $m=1$ cyclotron mode and diocotron mode frequencies. (a) The timing of the measurements. (b) Cross-plot of the two frequencies.

the diocotron mode frequency immediately following this burst by applying a similar low-frequency burst to a dipole section and adjusting its frequency so as to maximize the amplitude of the signal received on the second dipole section at the end of the burst. The timing of these bursts is illustrated in Fig. 5(a). Since the plasma is produced repetitively at about 5 Hz, these measurements are relatively straightforward. There is an uncertainty in the measured frequencies of at least 1 kHz because of the limited burst duration and some additional error results from shot-to-shot variation in plasma production.

Figure 5(b) shows a cross-plot of the frequency of the $m=1$ cyclotron mode versus the frequency of the $m=1$ diocotron mode obtained by making these measurements at various times in the plasma decay. From this plot, we conclude that the *downshift of the $m=1$ cyclotron mode from the cyclotron frequency is equal to the $m=1$ diocotron frequency,* to within experimental error.

One can understand this result from a simple model which ignores the internal degrees of freedom of the column, i.e., by treating the column, whatever its density profile, as undergoing a small rigid displacement. While the neglect of the internal degrees of freedom is an oversimplification, an analysis of a rotating fluid which includes all the internal degrees of freedom gives the same result.[14] Figure 6 shows the column displaced by a *small* amount δ_x from the axis of the surrounding conducting cylinder. This causes a redistribution of charges on the conductor, which in turn produces a uniform electric field E_x inside the cylinder whose value is given in Fig. 6. At low frequencies, the inertial terms can be neglected and this field results in a $E\times B$ drift of the charge distribution around the axis at the diocotron frequency ω_d. At high frequencies the most important force is the $v\times B$ force, with the induced electric field causing a small correction. Since the electric force is antiparallel to the $v\times B$ force it gives rise to a slightly reduced frequency of circular motion, or downshift. These effects are evident in the equations of motion of the rigid cylinder of charge:

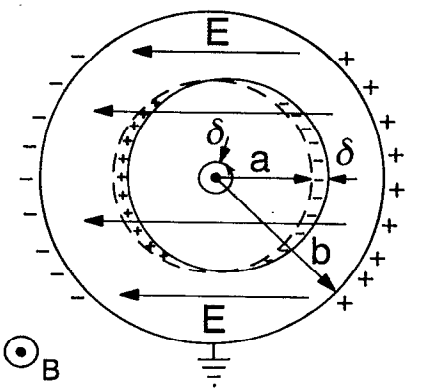

FIG. 6. Sketch showing electric field generated by a small rigid displacement of the plasma by δ_x from the axis.

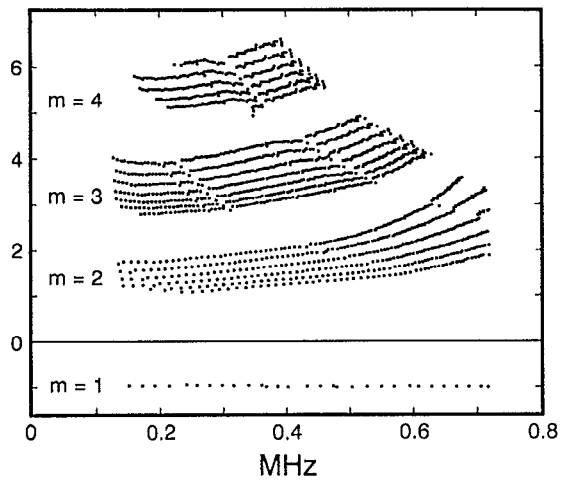

FIG. 7. Normalized frequency shifts, $(f-f_c)/f_d$, versus density, $f_d = \langle f_p^2\rangle/2f_c$ from the experimental data of Fig. 4. The rightmost and leftmost points correspond to the beginning and end of the trap cycle, respectively.

$$\ddot{\delta}_x+\omega_c\dot{\delta}_y=\tfrac{1}{2}\langle\omega_p^2\rangle\delta_x, \tag{2a}$$

$$\ddot{\delta}_y-\omega_c\dot{\delta}_x=\tfrac{1}{2}\langle\omega_p^2\rangle\delta_y. \tag{2b}$$

The right-hand side expresses the effect of the electric field of the wall charges. Equations (2a) and (2b) have both a low-frequency solution, which describes the $m=1$ diocotron mode, and a high-frequency solution, which describes the downshifted $m=1$ cyclotron mode. It is readily shown that the *sum* of these two frequencies is ω_c, in accord with our measurements. Since the magnitude of the induced electric field is the same for both modes, it is not surprising that the downshift of the $m=1$ cyclotron mode turns out to be equal to the diocotron frequency ω_d.

Having shown that the downshift of the frequency of $m=1$ cyclotron motion is the same as the $m=1$ diocotron frequency, we use the former rather than the latter to determine the mean density. A least-square two-exponential fit to the downshift was actually used to obtain the density decay shown in Fig. 3. Using the mean density, or more precisely the diocotron frequency ω_d, we normalize the frequency *shifts* of the various modes shown in Fig. 4 to $\langle\omega_p^2\rangle/2\omega_c$. These normalized shifts are plotted in Fig. 7 versus mean density. As would be expected from this normalization the $m=1$ shift is at -1.

IV. QUADRUPOLE MODES AND HIGHER, $m\geqslant 2$

From Fig. 7 we see that the normalized shifts of the $m=2,3,4$ modes fall into bands of approximately equally spaced resonances lying just below the values 2, 4, and 6, respectively. At early times, or high density, the shifts are slightly larger. In all scans taken, the normalized shifts fall into these bands, but the early time behavior and values of the normalized shifts may vary slightly from scan to scan.

We explain these bands as radially trapped, azimuthally propagating, Bernstein waves. Bernstein waves arise out of finite Larmor radius effects due to the nonzero electron temperature.[15] The fact that they are radially trapped follows from the radial angular velocity profile and the Doppler shift which it produces. We now present an approximate theory of radially trapped modes in a rotating pure electron plasma which is an *adaptation* of the Bernstein theory for plane waves in a neutral plasma. We start from the approximate plane wave dispersion relation for a spatially uniform plasma at rest when the frequency is close to the cyclotron frequency,[8]

$$\omega^2\approx\omega_c^2+\omega_p^2(1-k^2\rho^2/2). \tag{3}$$

It has also been assumed that $\omega_p^2 \ll \omega_c^2$ and $k^2\rho^2\ll 1$, where k is the wave number and ρ^2 is the mean square Larmor radius. To adapt this dispersion relation to a rotating non-neutral plasma two important changes are required. First, ω should be understood as, and therefore replaced by, the Doppler shifted frequency $(\omega-m\omega_0)$ seen by the rotating plasma (ω being the frequency in the laboratory). Second, ω_c should be understood as the single particle gyration frequency which, in a rotating non-neutral plasma, is slightly different from eB/m due to centrifugal and Coriolis effects.[14,16] To effect this correction we make the substitution, $\omega_c^2 \to (\omega_c - 2\omega_0)(\omega_c - 2\omega_0 - r\,d\omega_0/dr)$. Thus Eq. (3) becomes

$$(\omega-m\omega_0)^2-(\omega_c-2\omega_0)\left(\omega_c-2\omega_0-\frac{r\,d\omega_0}{dr}\right)$$

$$-\omega_p^2\left(1-\frac{k^2\rho^2}{2}\right)\approx 0. \tag{4}$$

Furthermore, we wish to apply this to a situation in which ω_0 and ω_p^2 are, in general, functions of radius and we will describe the r dependence through the dimensionless profile functions $g(r)$ and $f(r)$ introduced earlier. Since the frequency ω is given, we think of Eq. (4) as one which determines the local wave number of Bernstein waves in a plasma whose properties vary with radius slowly on the scale of a wavelength, i.e., $ka\ll 1$. In making this last approximation we are neglecting mode coupling and thus the coupling of the internal Bernstein modes to the external fields.[17] However, little error is made in the *frequencies* of the modes. In Eq. (4), the two leading terms in ω_c^2 cancel, and to first order in ω_0/ω_c, which is small, the remaining terms can be rearranged to give,

$$k^2=2[(m-1)g(r)-\lambda]/\rho^2 f(r), \tag{5}$$

where $\lambda=(\omega-\omega_c)/\omega_0(0)$ is a frequency shift, normalized to the *central rotation frequency,* which is proportional to the *central* density. From Eq. (5) and the fact that $g(r)$ decreases monotonically with radius from unity on the axis, we see that k^2 can pass through zero and change sign at a critical radius. Thus there are propagating waves inside the critical radius and evanescent waves outside the critical radius. This situation will occur when $(m-1)>\lambda>(m-1)g_{\min}$ since $g_{\max}=1$. To obtain the allowed values the normalized resonant frequencies λ, we convert Eq. (5) to a differential equation in cylindrical coordinates, $(1/r)d(rR)/dr-m^2R/r^2+k^2R=0$, and solve it numerically; $R(r)$ is proportional to the perturbed

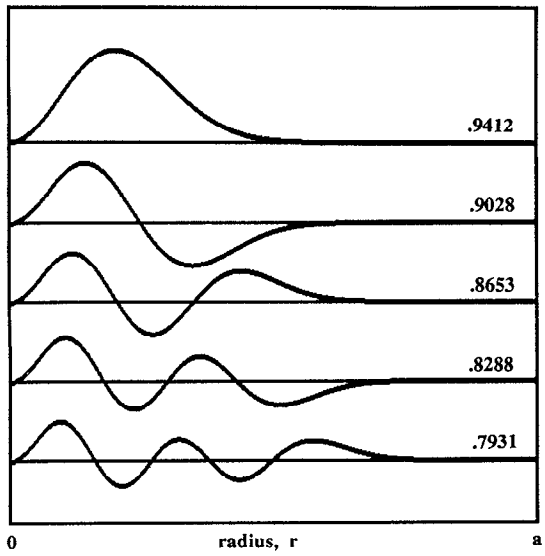

FIG. 8. Radial wave functions for $m=2$, $\rho/a=0.02$, with their normalized frequencies. The first five modes are shown.

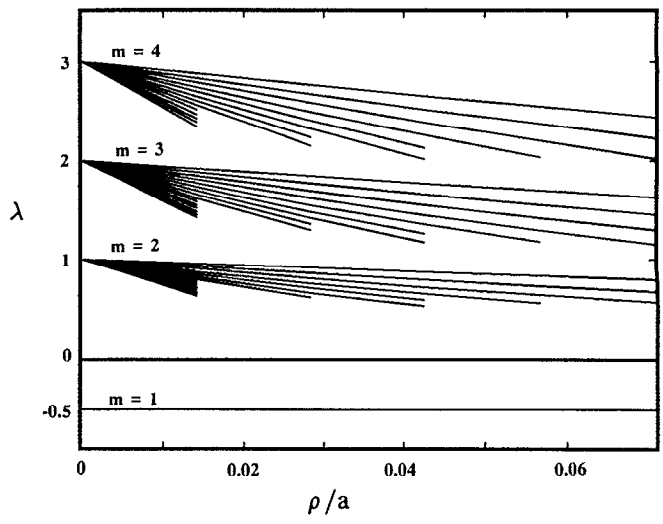

FIG. 9. Theoretical spacing of trapped $m=2$ Bernstein modes versus Larmor radius, ρ/a, normalized to the *central* rotation frequency $f_p^2(0)/2f_c$, for the profiles of Fig. 2.

density.[17] We use the profile functions described in Fig. 2 and note that the resulting eigenvalues will be insensitive to the details of the profile functions beyond the critical radius and therefore at the conducting wall. Near the origin, $R\sim r^m$ and beyond the turning point $R\to 0$. Examples of the first few solutions for $\rho/a=0.02$ are shown in Fig. 8, with the corresponding normalized frequency shifts, λ. As the radial mode number l increases, the critical radius increases so as to accommodate more nodes in the eigenfunction, and the frequency shift decreases. The *differences* in normalized frequency are nearly constant. These differences decrease with decreasing ρ/a as shown in Fig. 9. In the limit $\rho/a\to 0$ the modes become dense. By comparing the experimentally measured mode spacings with the results shown in Fig. 9 a value of ρ/a for the experiment can be inferred.

When the modes are trapped close to the axis, $f(r)\approx 1$ and the differential equation has the same form as the two-dimensional harmonic oscillator equation. The eigenvalues of the simplified equation can be shown to be

$$\lambda_{lm}=m-1-\sqrt{m-1}(2l+m-1)(\rho/a), \qquad (6)$$

where $l=1,2,3,...$ is the radial mode number. For the lowest l values Eq. (6) is in good agreement with the numerical results of Fig. 9.

By comparing the experimentally observed values of the frequency shifts with the predictions of Eq. (6) or of Fig. 9, we can infer certain properties of the plasma. Since ρ/a is small, Eq. (6) gives a series of closely spaced modes whose normalized shifts lie just below $m-1$, where m is the azimuthal mode number. By comparing the experimentally observed mode spacings for a given m with the predictions of Eq. (6), ρ/a can be determined and from the data of Fig. 4 it is found to be about 0.04. Since the theoretical shifts of Eq. 6 have been normalized to the central rotation frequency, $\omega_p^2(0)/2\omega_c$, the upshifts of the various series limits from the cyclotron frequency also give a good approximation to the central rotation frequency. Now the experimental data was normalized to the $\langle\omega_p^2(r)\rangle/2\omega_c$ and the series limits of the experimental shifts fell at about 2, 4, 6, for $m=2,3,4$, respectively. Comparing this with the theoretical limits of 1,2,3, respectively, we infer that the ratio of central density to mean density of the plasma is about 2. While this is not sufficient to determine the density profile completely, it is consistent with our assumed profile if the parameter a is taken to be the radius of the conducting wall. If this were the case, our previously inferred value of ρ/a gives an electron temperature of about 2 eV.

V. SUMMARY

In this experiment we have shown that there is a rich structure of modes in a rotating non-neutral plasma column close to the cyclotron frequency in a low-density plasma. We have also shown that frequencies of these modes are shifted away from the cyclotron frequency by amounts that are proportional to density. The $m=1$, $k_z\approx 0$ mode is found to be downshifted from the cyclotron frequency by an amount equal to the diocotron frequency, and we have given a simplified explanation of this result, a result which is also born out by the fluid theory. For each m greater than 1 we find a series of eight to ten closely spaced modes of diminishing amplitude, upshifted from the cyclotron frequency by amounts roughly proportional to $m-1$. We interpret these modes as radially trapped, azimuthally propagating, thermal Bernstein modes which arise out of finite Larmor radius effects. The origin of the upshift of their frequency is Doppler shift due to rotation. Radial trapping results because the angular velocity profile decreases with radius from the axis. By comparing the experimental results with a simplified theory, we can infer the ratio of electron Larmor radius to plasma scale length and we can determine the rotational angular velocity on axis.

VI. DISCUSSION

The radially trapped Bernstein modes in a non-neutral plasma column are similar in some respects to the $m=0$ Buchsbaum–Hasegawa modes[11] in a neutral plasma column with a radial density profile. However, there are a number of important differences, the most important of which arise from plasma rotation. First, the origin of the trapping can be traced to the angular velocity profile, rather than the density profile although the two are related. Also there is a frequency upshift due to azimuthally propagating modes in a rotating plasma. This gives the Doppler shift proportional to m and to the angular velocity. Finally, the modes are observed near the cyclotron frequency, rather than near the second harmonic of the cyclotron frequency.

The modes we observe appear to have $k_z=0$. Driving one segment of one octupole section 180° out of phase with the same segment of the other octupole section should excite modes which are antisymmetric about the midplane. The lowest of these has $k_z \approx \pi/L$, where L is the length of the column. This mode, if excited, could be received with a similar arrangement with a different pair of segments. We do not see this mode, and we believe that this is because of cyclotron damping. The parameter, $(\omega-\omega_c)/k_z v_{\text{th}}$, which governs cyclotron damping[8] would be of order unity so damping of this mode should be large.

Bernstein modes for $m=1$ are conspicuous by their absence. We note that $m=1$ is a special case, and Eq. (5) simplifies to $k^2=-2\lambda/\rho^2 f(r)$; k^2 is positive, and therefore waves propagate, for all radii so long as λ is negative. There is no longer a critical radius at which waves are reflected. However, k^2 becomes very large at the plasma edge where the density becomes very small and the waves are likely to be absorbed there rather than reflected.

Finally, we point out that the rigid-rotor equilibria, often used in theoretical studies,[9,2,18,19] has an angular velocity that is independent of radius and therefore does not give rise to radially trapped Bernstein modes. Furthermore, the question of what happens to the Bernstein waves at the plasma edge of a rigid-rotor equilibrium, where the density falls smoothly to zero in a short distance (as discussed in the preceding paragraph for $m=1$), has not received attention in the kinetic treatment of waves in non-neutral plasmas.[9,2] This question also arises in slab equilibria.[16]

ACKNOWLEDGMENTS

The insights into the behavior of non-neutral plasmas of Fred Driscoll, John Malmberg, and Thomas O'Neil were very helpful in the early stages of this work.

We are pleased to acknowledge the support of the U.S. Office of Naval Research and the assistance of Sateesh Pillai in the conduct of this research.

[1] *Non-Neutral Plasma Physics,* AIP Conf. Proc. 175, edited by C. W. Roberson and C. F. Driscoll (AIP, New York, 1988).
[2] R. C. Davidson, *Physics of Nonneutral Plasmas* (Addison–Wesley, Redwood City, CA, 1990).
[3] A. W. Hyatt, C. F. Driscoll, and J. H. Malmberg, Phys. Rev. Lett. **59**, 2975 (1987); J. H. Malmberg, Bull. Am. Phys. Soc. **36**, 2271 (1991).
[4] K. S. Fine, C. F. Driscoll, and J. H. Malmberg, Phys. Rev. Lett. **63**, 2975 (1989).
[5] C. F. Driscoll and J. H. Malmberg, Phys. Rev. Lett. **50**, 167 (1983); see also C. F. Driscoll, K. S. Fine, and J. H. Malmberg, Phys. Fluids **29**, 2015 (1986).
[6] G. Gabrielse, X. Fei, L. A. Orozco, R. L. Tjoelker, J. Haas, H. Kalinowsky, T. A. Trainor, and W. Kells, Phys. Rev. Lett. **65**, 1317 (1990).
[7] R. S. Van Dyck, Jr., F. L. Moore, D. L. Farnham, and P. B. Schwinberg, Phys. Rev. A **40**, 6308 (1989). Here an ion number dependency which is important for sub-ppb accuracy is pointed out.
[8] For a good review of Bernstein waves in neutral plasmas, see G. Bekefi, *Radiation Processes in Plasmas* (Wiley, New York, 1966).
[9] R. C. Davidson and N. A. Krall, Phys. Rev. Lett. **22**, 833 (1969); Phys. Fluids **13**, 1543 (1970).
[10] R. W. Gould and M. A. LaPointe, Phys. Rev. Lett. **67**, 3685 (1991).
[11] S. J. Buchsbaum and A. Hasegawa, Phys. Rev. Lett. **12**, 685 (1964); Phys. Rev. **143**, 303 (1966).
[12] J. S. DeGrassie and J. H. Malmberg, Phys. Fluids **23**, 63 (1980).
[13] R. H. Levy, Phys. Fluids **11**, 920 (1968).
[14] R. W. Gould, submitted to Phys. Fluids B.
[15] I. B. Bernstein, Phys. Rev. **109**, 10 (1958).
[16] S. A. Prasad, G. J. Morales, and B. D. Fried, Phys. Fluids **30**, 3093 (1987).
[17] Gary A. Pearson, Phys. Fluids **9**, 2454, 2464 (1966).
[18] D. H. E. Dubin, Phys. Rev. Lett. **66**, 2076 (1991).
[19] S. A. Prasad and T. M. O'Neil, Phys. Fluids **26**, 665 (1983); **27**, 206 (1984).